# Poly (ether sulfone) (PES)/polystyrene (PS) Thermoplastic Polymer Blend: Molecular Dynamics (MD) Simulation Methods and Experimental to Miscibility Evaluation

[1]Fateme Kouhestani, [2]MohamadAli Torangi*, [1]Alireza Motavalizadehkakhky
[3]Reza karazhyan and [4]Rahele Zhiani
[1]*Department of Chemistry, Neyshabur Branch, Islamic Azad University, Neyshabur, Iran.*
[2]*Department of Polymer Engineering, Faculty of Engineering, Golestan University, Gorgan, Iran.*
[3]*Industrial Biotechnology on microorganisms department. ACECR, Mashhad, Iran.*
[4]*Department of chemistry, Islamic Azad University, Neyshabur Branch,*
*Young and Elite Research Club, Neyshabur, Iran.*
m.torangi@gu.ac.ir*

(Received on 31st March 2023, accepted in revised form 29th August 2023)

**Summary:** In this study, poly (ether sulfone) (PES)/polystyrene (PS) thermoplastic polymer blend miscibility was looked at using both molecular dynamics (MD) simulations and experiments. In particular, the parameters of the Flory-Huggins interaction and the heat of mixing of poly (ether sulfone) (PES)/polystyrene (PS) blends at different compositions were calculated from MD simulation. For the PES/PS blend, both differential scanning calorimetry (DSC) and MD simulation showed that they are immiscible at PES/PS: 80/20,60/40 ratios. The degree of compatibility of the 20/80 and 40/60 PES/PS blends is higher than that of a PES-rich blend. This thermodynamic behavior was found to be due mainly to intermolecular interactions. Scanning electron microscopy (SEM) results confirmed this observation. Results show that the calculated $\chi$ value is positive at the compositions of PES/PS: 80/20 and 60/40, which confirmed that the polymer mixtures were immiscible at these compositions. The miscibility between PES and PS at these ratios is attributed to favorable van der Waals interactions. Also, the results of the DREIDING 2.21 force field show that electrostatic energy, bond angle bending energy, and bond stretching energy may be to blame for the immiscibility of certain composition polymer blends (PES/PS: 80/20 and 60/40).

**Keywords:** Miscibility; Poly (ether sulfone) (PES); Polystyrene (PS); Molecular dynamics simulation.

## Introduction

Thermoplastic polymers, which have garnered increasing attention, encompass a wide range of applications, including machine components, consumer items, membrane separation, storage materials and packaging, and medical equipment [1–4]. In recent years, engineered blends of thermoplastic polymers have gained growing significance in the polymer market. The prediction and description of blend miscibility have attracted significant focus to optimize the design of these compositions. Polymer blending is frequently employed to enhance physical properties and expand the potential applications of a given polymer [5-9]. Within polymer blends, the macroscopic characteristics are intricately tied to the microstructure of the system, primarily contingent upon the miscibility and compatibility of the components. Not only pivotal for polymer blends, miscibility plays a determining role in the physical characteristics of copolymers and interpenetrating networks, offering insights into the potential commercial uses of these polymer combinations [10, 11].

Numerous methodologies exist to determine blend miscibility in polymer blends. Observation through microscopy [12], the Tg method [13], Dilute Solution Viscometry [14], the Hildebrand Solubility Parameter Approach [15], Melting Point Depression Method [16], Molecular Dynamics (MD) Simulation [17], and Small Angle Neutron Scattering (SANS) Method [18] have all been employed in preliminary investigations of miscibility.

One of the primary objectives of this research is to gain insights into the molecular-level miscibility of PES/PS thermoplastic polymer blends, leveraging Molecular Dynamics simulations. A fundamental understanding of the thermodynamics of polymer blends necessitates precise knowledge of their chemical structures and local packing behaviors. The research aims to provide guidance regarding the relationship between miscibility and chemical structure in polymer blends, with the intention of generating actionable data. This study determined the heats of mixing and corresponding Flory-Huggins interaction parameters for various binary blends using

*To whom all correspondence should be addressed.

MD simulations. The glass transition temperature is intrinsically linked to blend miscibility and is a crucial determinant in assessing a polymer's suitability for specific applications. However, the glass transition remains one of the most enigmatic properties of polymers. Furthermore, the study aims to create a novel and accurate methodology for predicting the glass transition temperatures of polymers solely based on their chemical structure, utilizing molecular dynamics simulations.

## Experimental

### *Materials*

Poly (ether solfun) (PES) (molecular weight = 58000 gr/mol, specific heat = 1100 J/Kg/K, density = 1.4 g/Cm$^3$, and $T_g$ = 220 °C) and poly (styrene) (PS) (molecular weight = 35000 gr/mol, specific heat = 1230 J/Kg/K, density = 1.05 g/Cm$^3$ and $T_g$ = 370 °C) were purchased from Sigma-Aldrich. All materials were provided in pellet form. Prior to usage, a vacuum oven was used to dry PES and PS for 4 hours at 50 °C. Dimethylacetamide (DMAc) with high purity and analytical grade was used as the solvent, supplied by Merck.

### *Experimental methods*

### *Melt Blending of PES/PS*

A mixer, RHEOMIX 600P type 557-1302, was used for PES/PS polymer blend preparation. The combined weight of the components is required to have a total melt volume of 72% of the volume of the mixing chambers. All the experiments are performed at 50 rpm, which corresponds to a 65 s-1 shear rate at the minimum gap of the mixer. In order to reduce degradation during melt mixing, 0.1 wt% tris (2,4-di-tertbutylphenyl)-phosphite (Sumchun, Korea) as the stabilizer was added to the blends. The PES/PS blend ratios we prepared in this study were: 80/20; 60/40; 40/60; and 20/80. In this regard, PES and PS polymers were placed in the mixer. Following that, a weight of five kilograms was positioned atop the ram, and the ram was then positioned above the chambers.

For PES-rich phase blends, the PES pellets were added first, and the PS pellets were added 2 minutes later, when the PES pellets were already melted. The 10 minutes of mixing time are sufficient to achieve a fine mix. After mixing, a sample was quenched in liquid nitrogen.

### *Film preparation*

At first, blends of two polymers were prepared with various compositions in weight ratios of PES/PS: 80/20, 60/40, 40/60, and 20/80, ($T$: 25°C). After pouring these mixtures onto a glass plate, the solvent was permitted to evaporate. The resultant films were dried at 50 degrees Celsius for 24 hours.

### *Characterization*

The samples' glass transition temperatures were measured using a differential scanning calorimeter (DSC-60 A Plus model, Shimudza company, Japan) at a nitrogen environment from 0 to 400 degrees Celsius at a rate of 10 degrees Celsius per minute.

SEM images were made with a JSM-IT500HR InTouchScope Scanning Electron Microscope with a 26 kV accelerating voltage.

The spectrum was obtained on a Nicolet iS50 FTIR spectrometer in the region of 600-4000 $cm^{-1}$.

### *Molecular dynamics simulation details*

### *DREIDING 2.21 force filed*

For various physical systems, a huge number of parameterized force fields have been developed. In this research, MD simulations of polymers were performed using the DREIDING 2.21 force field. Cerius2, in its 4.6 edition, is a commercial software product that was utilized for this goal. According to DREIDING 2.21, the sum of bonding and non-bonding interactions characterizes the overall energy of a system:

$$E = E_b + E_\theta + E_\emptyset + E_\varphi + E_{VDW} + E_Q \qquad (1)$$

where $E_b$ is the bonded interactions, $E_\theta$ is the bond angle bending, $E_\emptyset$ is the torsion angle rotations, $E_\varphi$ is the tetrahedral center inversions, $E_{VDW}$ is the non-bonded interactions, and $E_Q$ is the electrostatic energies.

The bond-stretching energy is described by a harmonic oscillator:

$$E_b = \frac{1}{2} k_b (l - l_0)^2 \qquad (2)$$

In this equation $E_b$ is the bond stretching energy, $l$ is the bond length, and $l_0$ is the equilibrium bond length. The bond bending energy calculated by Eq.3 is:

$$E_\theta = \frac{1}{2} k_\theta (cos\theta - cos\theta_0)^2 \qquad (3)$$

where $\theta$ is the bond angle between two adjacent bonds and $\theta_0$ is the equilibrium bond angle. Torsional energy

describes the interaction between two bonds joined by a common bond, given by Eq. 4:

$$E_{\emptyset} = \frac{1}{2}k_{\emptyset}\{1 - \cos[n(\emptyset - \emptyset_0)]\} \quad (4)$$

where $\emptyset$ and $\emptyset_0$ are torsional angle and equilibrium torsional angle, respectively, $k_{\emptyset}$ is the obstacles to rotation, while $n$ is an integer and is the periodicity. Inversion energy in the Dreiding force field takes the form:

$$E_{\varphi} = \frac{1}{2}k_{inv}(\varphi - \varphi_0)^2 \quad (5)$$

where $\varphi$ is the plane angle and $\varphi_0$ is defined as zero for a plane molecule. For nonbonded interactions, *EVDW* is defined by means of a Lennard-Jones equation:

$$E_{vdw} = D_0\left[\left(\frac{R_0}{R}\right)^{12} - 2\left(\frac{R_0}{R}\right)^{6}\right] \quad (6)$$

In this equation, $R$ is the van der Waals interaction distance, $D_0$ is the van der Waals energy well depth, and $R_0$ is the van der Waals bond length.

The electrostatic energy is calculated as follows [19]:

$$E_Q = 332.063\frac{q_i q_j}{\varepsilon R_{ij}} \quad (7)$$

In this equation, $qi$ and $qj$ are the partial charges of atoms i and j, respectively. $Rij$ is the space among them and $\varepsilon$ is the dielectric constant. In DREIDING 2.21 force field, a distance dependent dielectric constant was used.

*Simulation details*

The simulation details for building the PES/PS blend model are given in Table 1. After blend construction, the blend systems were checked to make sure that the various component chains blended well together. If the first configuration didn't mix the two component chains well, it was thrown out and a new configuration was tried. Different initial conformations were built and subjected to energy minimization. The conformation with the lowest potential energy was selected to be used for the following MD simulation. In order to avoid the structure being trapped in a local minimum, after energy minimization, a high-temperature MD simulation was employed, followed by energy minimization.

In this study, the amorphous cells of pure polymers and polymer blends were equilibrated at 1,000 K for 100 ps using an NVT ensemble. The snapshot with the lowest energy was chosen, and its energy was further reduced until the derivatives were less than 0.1 kcal.mol$^{-1}$.

*MD simulation of polymer blends*

Two polymers, with degrees of polymerization $N_A$ and $N_B$, will be miscible if their Flory-Huggins interaction parameter is less than $(\chi_{AB})_{cri}$ that given by:

$$(\chi_{AB})_{cri} = \frac{1}{2}\left(\frac{1}{\sqrt{N_A}} + \frac{1}{\sqrt{N_B}}\right)^2 \quad (8)$$

The estimation of mixing enthalpy change is a common approach for binary polymer systems for determining the Flory-Huggins interaction parameter. Several approaches for predicting the enthalpy of mixing have been presented. One experimentally available method is using low-molecular-weight compounds whit chemical structures closely related to those of the polymer-repeating units. However, because chain segments are bound and the additional steric hindrances experienced by the polymers are rather different from those of compounds with a low molecular weight, MD simulation provides a direct method to determine the mixing enthalpy. Also, the heat change of mixing can be predicted by the difference between pure polymers and blends enthalpies according to the following equation.

$$\Delta H_m = H_{mixture} - \sum n_i H_i \quad (9)$$

where $H_i$ is the enthalpy of pure components and blend system's enthalpy denoted by $H_{mixture}$.

Table-1: Simulation details of the PES/PS blend system.

| label | Composition (PES/PS) | Density of the system ($gr/cm^3$) | Molar volume ($cm^3/mol$) | $\chi$ |
|---|---|---|---|---|
| 1 | 100/0 | 1.4 | 6324.2 | N/A |
| 2 | 80/20 | 1.3 | 5322.2 | 2.66 |
| 3 | 60/40 | 1.27 | 6234.2 | 2.74 |
| 4 | 40/60 | 1.21 | 6201.2 | -0.98 |
| 5 | 20/80 | 1.13 | 5987.1 | -1.78 |
| 6 | 0/100 | 1.05 | 5176.5 | N/A |

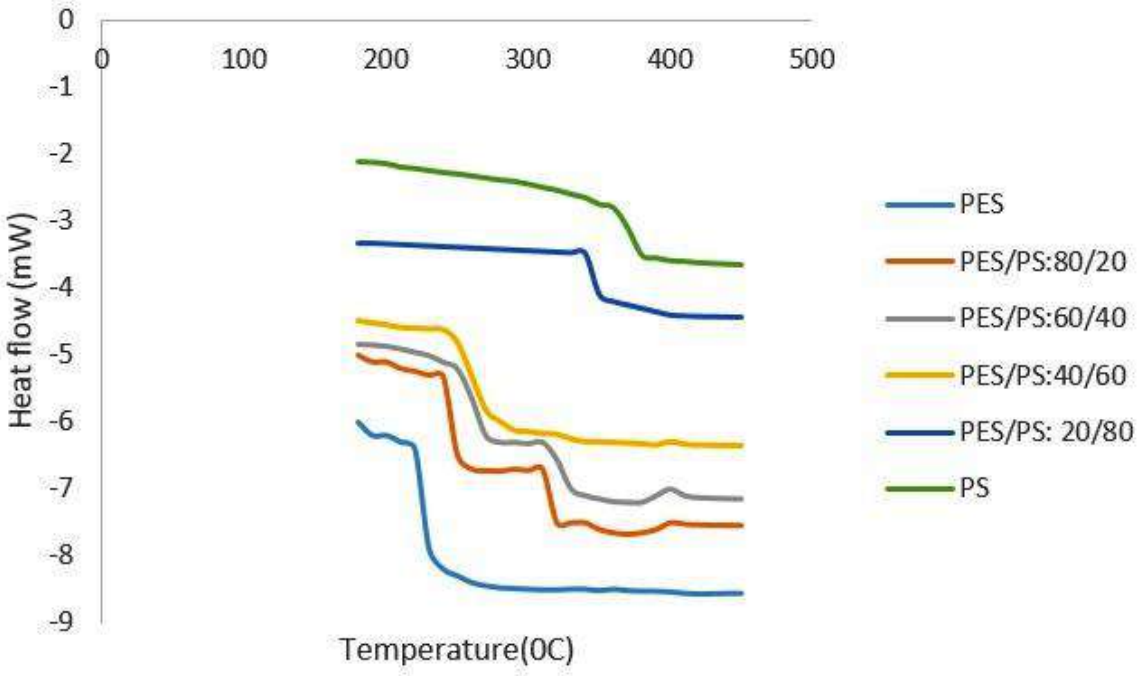


Fig.1: Heat flow versus temperature of PES/PS blends.

The Flory-Huggins interaction parameter can be calculated using the following equation:

$$\Delta H_m = {}^{\chi}RT\emptyset_1\emptyset_2 \qquad (10)$$

where $\emptyset_1$ and $\emptyset_1$ are the fractions of polymer 1 and polymer 2 by volume, respectively.

**Results and Discussion**

*DSC results*

In this section, we established two separate $T_g$s for PES/PS blends in ratios of 80/20 and 60/40 in the DSC measurements (see Fig 1), one for the PES-rich phase and one for the PS-rich phase, respectively. These polymers are immiscible because they have different Tg values. The two concentration dependents of Tg are shown in Figs 2 and 3, respectively. The Tg in these Figs is averaged from three parallel measurements. Fig. 2 indicates that the Tg of PS in the blends is the same as that of pure PS. However, Fig. 3 demonstrates that the Tg of PES in the blend first reduced with increasing PS amounts up to 20 wt%, then reached a low at 20% PS, and ultimately improved at higher PS values and reached the Tg of pure PES. At 80% PES, there was a maximum reduction in Tg of roughly 5 °C. According to DSC measurement, two different $T_g$'s were found in ratios of PES/PS: 80/20, 60/40 for the blend system (Fig 1). The presence of two different $T_g$'s confirms the immiscibility of the two polymers. The two concentration dependents of $T_g$ is shown in Figs 2 and 3, respectively. The $T_g$ in these Figs is averaged from three parallel measurements. Fig. 2 shows that the $T_g$ of the PS in the blends is not much different from the $T_g$ of PS in the pure state. Also, Fig. 3 indicates that the $T_g$ of PES in the blend decreased with increasing PS content to 20 wt% and then increased at higher PS contents.

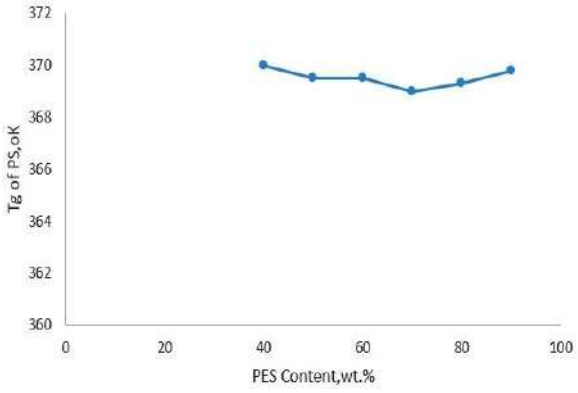


Fig. 2: Concentration dependence of $T_g$ of PS in PES/PS blends.

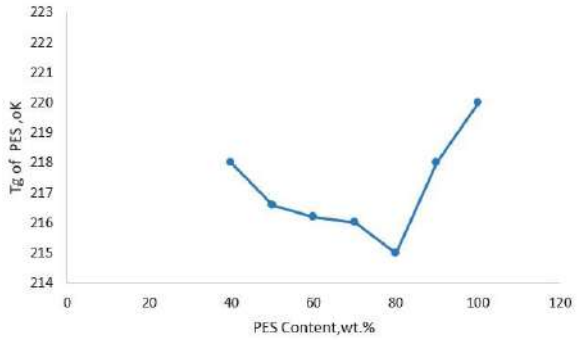


Fig. 3: Concentration dependence of $T_g$ of PES in PES/PS blends.

*SEM results of PES/PS blends*

The SEM analysis demonstrates the homogeneity of the film surfaces of pure PS and PES (fig. 4). Blends of PES/PS with PES/PS ratios of 20/80 and 40/60 demonstrate homogeneity, and it is obvious that PES is well dispersed in the PS matrix, but blends with other PES/PS ratios revealed clearly phase separation, indicating their immiscibility. As phase separation can be seen in the analyzed SEM images, it is determined that the 60/40 blend is only partially miscible. Therefore, it is possible to conclude that the composition blends of PES/PS (20/80) and (40/60) have acceptable PS and PES interactions.

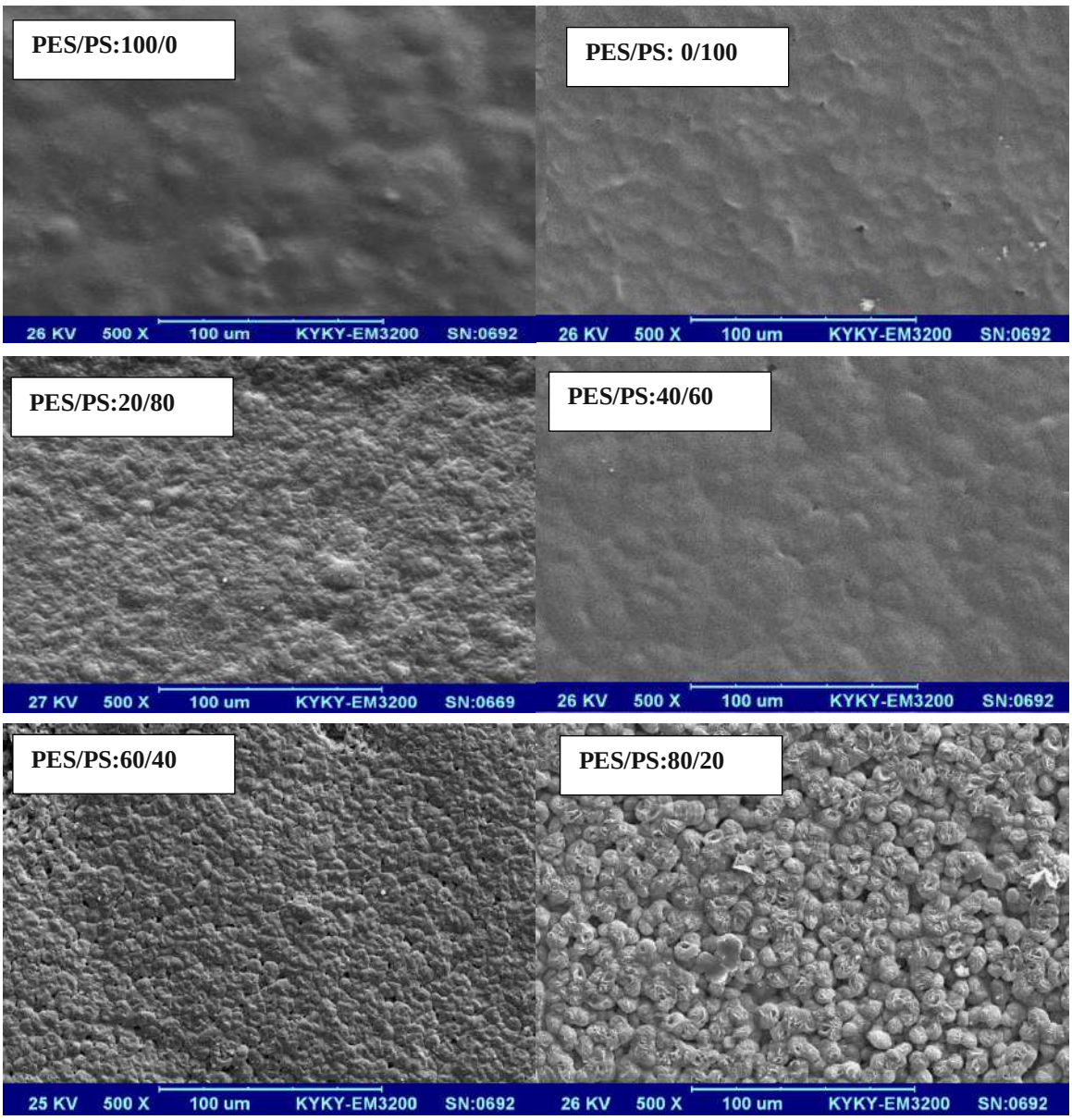


Fig.4. SEM result of surface morphology of PES/PS blend films.

*MD simulation results*

*Simulation of pure polymers*

Cohesive energy density is one of the most important thermodynamic properties of a liquid, and it is often used in the literature to validate the force field chosen for the simulation [20, 21]. Compared with small molecules, Polymer molecules have a vanishingly small vapor pressure, and the molar energy of vaporization cannot be determined directly from the experiment. MD simulation provides a direct method to determine the density amount of cohesive energy inside polymers, and the molar energy of vaporization can be determined from $\Delta E_v = E_{vac} - E_{Balk}$, where $E_{vac}$ and $E_{balk}$ are the potential energies of the system in a vacuum state and in bulk state, respectively. They can be calculated from MD simulations. It should be pointed out that the concept of the cohesive energy density of polymers is borrowed from the definition of small molecules; for polymers, because of the high internal degree of freedom, the configuration of a polymer chain in vacuum is not exactly the same as that of in the liquid state. In the analysis of simulation results, the CED was sampled every 10 ps for the last 100 ps of the NVT simulation.

By taking the square root of CED, we can get the solubility parameter. On display in Table 2 are the solubility parameters for PS and PES. In this Table, the solubility parameters predicted from the group contribution and solvent swelling methods are also listed for comparison purposes. Table 2 shows that the solubility parameter calculated based on the PCFF force field differs relatively much from the results obtained from the others. Table 2 shows that the solubility parameters of PS we obtained based on the COMPASS and DREIDING force fields are 18.5 and 19.9 $MPa^{1/2}$ respectively. They are fairly close to each other, and they match up well with the value derived from the group contribution technique. Group contribution technique values for PES solubility parameters are consistent with those obtained by DREIDING 2.21 and COMPASS force field calculations (22.8- 23.2 $MPa^{1/2}$).

According to the longer CPU time of the COMPASS force field in simulation, the DREIDING 2.21 force field was used for PES/PS blend simulation. Since the experimental density cannot be reproduced by this force field, it is inappropriate for the NPT ensemble. Also, the NVT ensemble, by using the DREIDING 2.21 force field, creates a lot of pressure in simulation.

Because of the limited computational resources, simulation cannot be done on the real polymer size.

Nevertheless, the size of the molecule is important in order to accurately calculate its thermodynamic properties. Because of this, it's important to have at least the bare minimum of molecules to indicate the real polymer. For this purpose, various parameters for PS and PES solubility were evaluated. The solubility parameters of PES and PS versus the number of repeating units are presented in Figs 5 and 6, respectively. Fig 5 indicates that the solubility parameter of PS decreases as the molecular weight increases. The solubility parameters of PES have a similar trend to those of PS. The simulation was continued with the PS molecule having 55 repeating units ($M_n = 5726$) and the PES molecule having 25 repeating units ($M_n = 5900$).

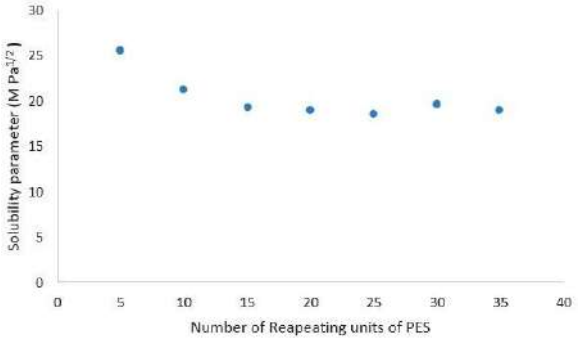


Fig.5. PES solubility parameter, as calculated, plotted against the number of repeating units.

Table-2: Solubility characteristics of PES and PS simulated by various force fields at 25°C.

| Name | Repeating units | MWT | Solubility parameter ($MPa^{0.5}$) | | | |
|---|---|---|---|---|---|---|
| | | | DREIDING 2.21 | PCFF | COMPASS | Calculated by group contribution method |
| PS | 55 | 5726 | 18.5 | 24.6 | 19.9 | 19.2 |
| PES | 25 | 5900 | 23.2 | 27.8 | 22.8 | 23 |

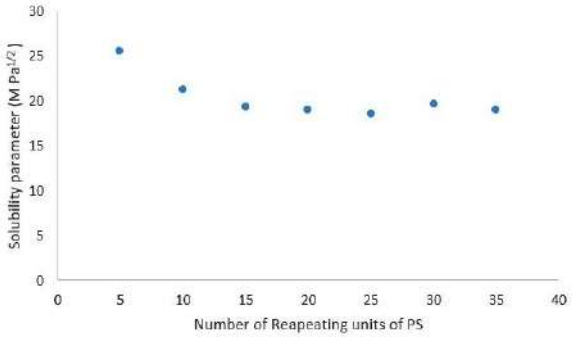


Fig. 6: PES solubility parameter, as calculated, plotted against the number of repeating units.

*MD simulation of PES/PS blends*

For each concentration in the blend, molecular dynamic path files were created using NVT. The simulation was run until a stable energy was attained, at which point the needed equilibrium time was calculated based on the system's size. After that, the time-averaged potential energy values in the final 100 ps of the path were used to determine the mean potential energies of the bulk and vacuum states.

For the blend systems, $\Delta H_m$m may be computed by noting that $\Delta H_m$ is about equal to $\Delta H_m$.

Table 3 provides a summary of the energy change that occurs during mixing for each different form of energy. Fig 7 is the plot of $\Delta H_m$ and $\Delta G_m$, versus weight fraction of PS. The $\Delta G_m$ was calculated from the following equation:

$$\Delta G_m = \Delta H_m - T\Delta S_m{}^{comb} \qquad (11)$$

where $\Delta S_m$ $comb$ is the combinational entropy changes. Fig. 7 shows that the $\Delta H_m$ and $\Delta Gm$ curves are similar. The $\chi$ values obtained by equations 9 and 10 are plotted versus weight percent of PS in Fig 8. The positive values of $\chi$ at composition of PES/PS: 80/20 and 60/40, indicate the immiscibility of two polymers at these compositions. This immiscibility is due to the bond angle bending energy, electrostatic energy, and bond stretching energy present in certain compositions. Also, as the weight percent of PS increases, change in the $\chi$ is observed. The majority of the shift in $\chi$ was attributable to van der Waals and electrostatic energy. In other words, van der Waals interaction is the main contribution to the miscibility of PES/PS blends at 40/60 and 20/80 compositions, which is in contrast to the fact that the van der Waals interaction is responsible for the immiscibility of PES/PS blends at: 80/20 and 60/40 compositions.

Table-3: Energy changes upon mixing (kcal/mol) for PES/PS blend systems.

| Composition PES/PS | $\Delta E_b$ | $\Delta E_\theta$ | $\Delta E_\emptyset$ | $\Delta E_{inv}$ | $\Delta E_{vdw}$ | $\Delta E_Q$ |
|---|---|---|---|---|---|---|
| **80/20** | **32.4** | **11.7** | **-8.7** | **-0.56** | **6.3** | **10.65** |
| **60/40** | **15.6** | **7.9** | **-10.1** | **-3.26** | **4.3** | **2.3** |
| **40/60** | **1.7** | **2.3** | **-0.04** | **2.26** | **-8.56** | **-4.07** |
| **20/80** | **-4.65** | **-3.76** | **2.3** | **3.45** | **-18.3** | **-12.3** |

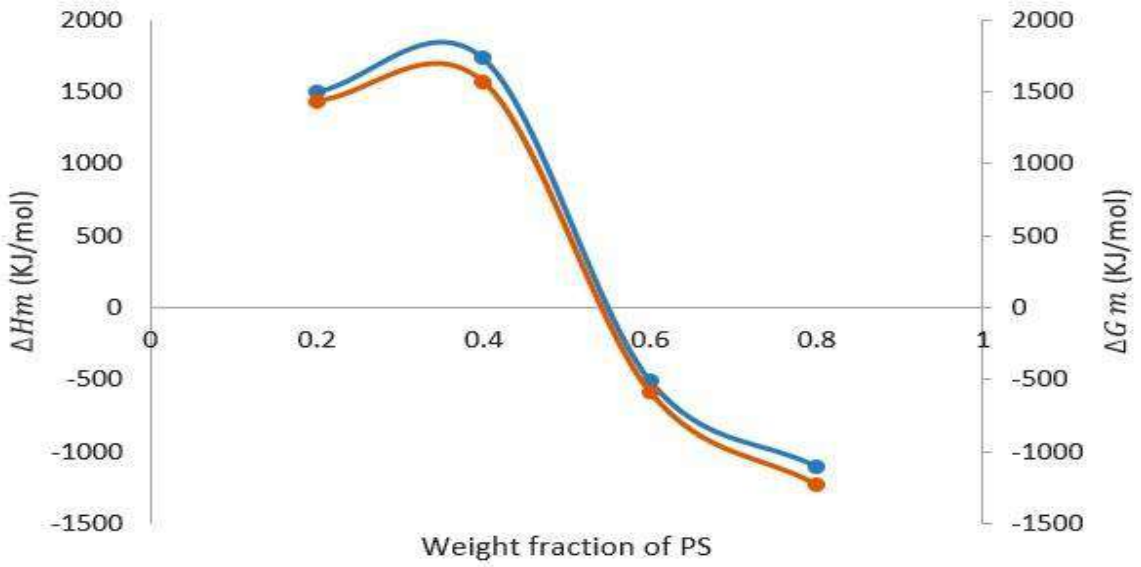


Fig. 7: Variations in molar enthalpy and Gibbs free energy upon mixing against PS weight fraction.

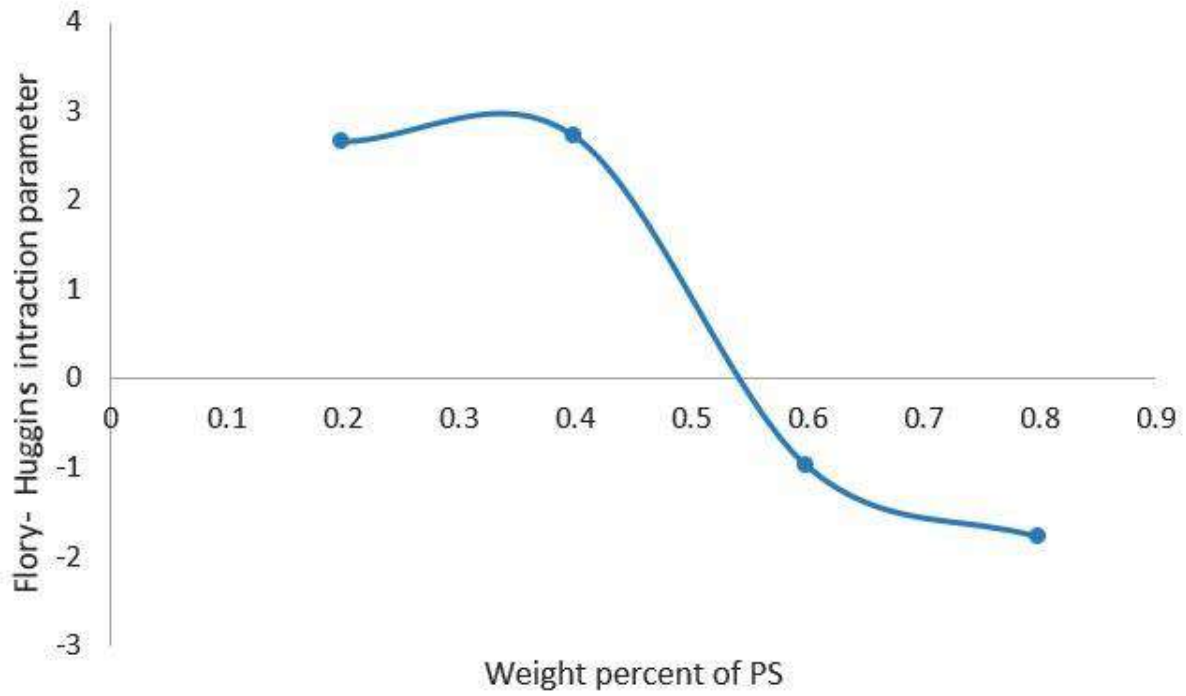


Fig. 8: Flory-Huggins interaction parameter versus volume fraction of PES/PS.

**Conclusion**

In this study, the thermal analysis and SEM results revealed the immiscibility of PES/PS blends in blend ratios of 80/20 and 60/40. By means of the DREIDING 2.21 force field, it also confirmed the immiscibility of these ratios. The simulated value of $\chi$ corresponds quantitatively to the value determined through experimental data. Understanding the fundamental causes behind the miscibility of PES/PS: 40/60 and PES/PS: 20/80 mixes was made possible using the NVT MD simulation. Our ability to do effective MD simulations of these engineering polymer blends will be further improved by a more efficient integration approach.

**Reference**

1. L. Y. Ljungberg, Materials selection and design for development of sustainable products, *Mater. Des.*, **28**, 466 (2007).
2. B. Khan, M. Bilal Khan Niazi, G. Samin and Z. Jahan, Thermoplastic Starch: A Possible Biodegradable Food Packaging Material—A Review, *J. Food Process Eng.* **40**, e12447 (2017).
3. X. Y. Zhou, Y. F. Cui, D. M. Jia and D. Xie, Effect of a Complex Plasticizer on the Structure and Properties of the Thermoplastic PVA/Starch Blends, *Polym Plast Technol Eng.*, **48**, 489 (2009).
4. P. Maheswari, P. Barghava and D. Mohan, Preparation, morphology, hydrophilicity and performance of poly (ether-ether-sulfone) incorporated cellulose acetate ultrafiltration membranes, *J. Polym. Res.* **20**, 1 (2013).
5. A. Graziano, S. Jaffer and M. Sain, Review on modification strategies of polyethylene/polypropylene immiscible thermoplastic polymer blends for enhancing their mechanical behavior, *J. Elastomers Plast.* **51**, 291 (2018).
6. F. Samadaei, M. Salami-Kalajahi, H. Roghani-Mamaqani and M. Banaei, A structural study on ethylenediamine- and poly(amidoamine)-functionalized graphene oxide: simultaneous reduction, functionalization, and formation of 3D structure, *RSC Adv.* **5**, 71835 (2015).
7. G. Ali, J. Nisar, M. Iqbal, A. Shah, M. Abbas, M. R. Shah, U. Rashid, I. A. Bhatti, R. A. Khan and F. Shah, Thermo-catalytic decomposition of polystyrene waste: Comparative analysis using different kinetic models, *Waste Manag. Res*. **38**, 202 (2020).
8. S. Rahim, S. Khalid, M. I. Bhanger, M. R. Shah and Malik, M. I., Polystyrene-block-poly (2-vinylpyridine)-conjugated silver nanoparticles as colorimetric sensor for quantitative determination of Cartap in aqueous media and blood plasma.

Sens. *Actuators B Chem.* **259**, 878 (2018).
9. J. Nisar, G. Ali, A. Shah, M. R. Shah, M. Iqbal, M. N. Ashiq and H. N. Bhatti, Pyrolysis of expanded waste polystyrene: Influence of nickel-doped copper oxide on kinetics, thermodynamics, and product distribution, *ENERG FUEL*. **33**, 12666 (2019).
10. A. Eckelt, J. Eckelt and B. A. Wolf, Interpolymer Complexes and Polymer Compatibility, Macromol. *Rapid Commun.* **33**, 1933 (2012).
11. R. Cardinaels and P. Moldenaers, Morphology Development in Immiscible Polymer Blends, *Polym. Morphol. Princ. Charact. Process.*, **348** (2016).
12. D. Feldman, Polyblend Compatibilization, *Journal of Macromolecular Science, Part A: Pure and Applied Chemistry*, **587** (2007).
13. M. Weber, Engineering polymer alloys by reactive extrusion, In Macromolecular Symposia, Weinheim: WILEY-VCH Verlag GmbH, p. 189 (2002).
14. M. Ebrahimpour, A. A. Safekordi, S. M. Mousavi and A. Heydarinasab, A miscibility study on biodegradable poly butylene succinate/polydioxanone blends, *J. Polym. Res.* **25**, 1 (2018).
15. M. Belmares, M. Blanco, W. A. Goddard, R. B. Ross, G. Caldwell, S. H. Chou, J. Pham, P. M. Olofson and C. Thomas, Hildebrand and Hansen solubility parameters from Molecular Dynamics with applications to electronic nose polymer sensors, *J. Comput. Chem.* **25**, 1814 (2004).
16. P. J. Marsac, S. L. Shamblin and L. S. Taylor, Theoretical and practical approaches for prediction of drug-polymer miscibility and solubility, *Pharm. Res.* **23**, 2417 (2006).
17. A. Takhulee, Y. Takahashi and V. Vao-soongnern, Molecular simulation and experimental studies of the miscibility of polylactic acid/polyethylene glycol blends, *J. Polym. Res.* **24**, 1 (2016).
18. O. Urakawa, H. Ikuta, S. Nobukawa and T. Shikata, Small-angle neutron scattering study on the miscibility and concentration fluctuation of hydrogen-bonded polymer blends, *J. Polym. Sci. Part B Polym. Phys.* **46**, 2556 (2008).
19. A. K. Rappé and W. A. Goddard, Charge equilibration for molecular dynamics simulations, *J. Phys. Chem.* **95**, 3358 (1991).
20. P. Gestoso and J. Brisson, Effect of hydrogen bonds on the amorphous phase of a polymer as determined by atomistic molecular modelling, *Comput. Theor. Polym. Sci.* **11**, 263 (2001).
21. M. Zhang, P. Choi and U. Sundararaj, Molecular dynamics and thermal analysis study of anomalous thermodynamic behavior of poly (ether imide)/polycarbonate blends, *Polymer (Guildf).* **44**, 1979 (2003).